STAR
Research Journal

Available online at www.starresearchjournal.com (Star International Journal)

PHYSICS

MORPHOLOGICAL AND VIBRATIONAL CHARACTERIZATIONS OF SnO_2 NANO MATERIAL USING COMPUTATIONAL CALCULATIONS

S. LAVANYA[1] & Dr. M.K. MURALI[2]

[1]*Ph.D Scholar, Department of Physics, J.J. College of Arts and Science, Pudukkottai, Tamilnadu, India.*
[2]*Assistant Professor & Head, Department of Physics, J.J. College of Arts and Science, Pudukkottai, Tamilnadu, India.*

Abstract

In this research work, SnO_2 Nano material was prepared using popular sol-gel combustion route. The XRD characterization was made along with the results obtained from the computational calculations. The inter planes of the crystals have been identified and the (000), (111), (222), (110), and (220) sequence of translational symmetry was keenly analyzed. The optimized parameters were calculated at different temperatures and they were compared with experimental results. The crystal lattice constants were calculated and the results were found to be supported the observed data. The Vibrational assignments made upon which the active compositional parts of the SnO_2 compound were recognized. The active IR and Raman bands of Sn-O bonds at different planes causing XRD peaks with maximum intensity were ensured. As the topographical effect of present nano system of particles was enabled, the molecular arrangement of crystal system was found to be having enriched surface area. The kubo gap of the prepared and the materials with annealing temperatures were determined and compared with calculated values at IR and UV-Visible regions. The light dispersion coefficient of the SnO_2 material was found and the relative parameters were calculated from the polarizability and hyperpolarizability constants. The frontier interactions profile was mapped and the cause of gas sensing property was studied.

Keywords: SnO_2, Raman bands, Sn-O, dispersion, Kubo gap, polarizability and hyperpolarizability.

1. INTRODUCTION

The systematic and sequential research in the field of nano scale metal oxide materials is motivated the nano scientist by the opportunity to process and design new synthesized nano structured fascinated materials with distinctive properties for ultimate important applications. Due to their equipped nano size and the manipulated surface-to volume ratio, well defined nano structured materials often show novel, and sometimes extraordinary properties [1]. The opto-electronic, thermo-electric, magneto-optical and forced nano-chemical properties customized in the nano materials in terms of much reduced size with oxygen vacancies [2]. In this way, the purposively designed nano sized metal oxide semiconductor material; SnO_2.

The SnO_2 is an n-type metal oxide semiconductor is having wide band gap around 3.80 eV due to which it has potential optical applications, particularly it is primarily used in gas sensors during the recent years[3]. The nano material of the metal oxide generally possessed good gas sensing characteristics since SnO_2 structurally having good sensitivity, optical selectivity and energy reproducibility [4-6]. The tetragonal lattice structured with large surface and squeezed edge atoms of SnO_2 provides active sites for catalyzing surface reactions. By the architecture, the SnO_2 materials are used in the fabrication of optoelectronic devices; LCD, LET transport conductors and solar–electrical energy transducers and toxic chemical and gas sensitive semiconductor devices.

However, the well defined nano structures to be investigated and analyzed by performing theoretical calculations using computational tools in order to study the customization of structural arrangement of the nano materials[7]. The computational parameters are generally providing the structural information by the understanding the optimized bond length, bond angle and dihedral angle. The Vibrational examinations over the bond length and angles of the molecular materials offered the active atomic sites and highly reflective planes of the nano crystal from which the entire crystal arrangement can be studied and the relative positions of the basic lattice [8]. From the observed data of geometrical parameters, the nano basic lattice formation of the nano structure can be identified and predicted and also the oxygen combinations in the lattice can be viewed.

After the thorough investigations made on previous works, no work related to computational analysis on SnO_2 nano materials was found. Hence, in this work, the optimized structure was predicted and the associated active crystal planes for X-ray reflections were recognized. The Vibrational spectra of FT-IR and FT-Raman tools were recorded and their Vibrational pattern was mapped. The Vibrational assignment of spectral pattern illustrated the active bonds in different planes and consumption of energy was noticed to describe the core symmetry.

2. SPECTRAL INFORMATION

The nano SnO_2 powder was prepared using sol-gel combustion technique and it was annealed different temperatures. In order to study the Vibrational pattern, the FT-IR and FT-Raman spectra were recorded on macro and nano samples with different scanning speed. For obtaining spectral data, the Bruker IFS 66V spectrometer was used for recording spectrum in the range of 1500–50 cm^{-1}. The FT-Raman spectra of nano powder was also recorded in the same instrument with FRA 106 Raman module equipped with Nd:YAG laser source operating at 1.064 µm line widths with 200 mW power.

3. COMPUTATIONAL PROFILE

In the case of nano samples at 200º, 400º and 600ºC, the structural parameters were obtained by performing the computational calculations by Gaussian 09 D. 01.version software program using iMac 7th Gen computer [9]. Most appropriate calculations were carried out for obtaining optimized structure data. The electrophilic and nucleophilic influence province, electrostatic potential field spreading and electronic orbital overlapping arrangments were visualized by performing calculations with higher order hybrid theories [10]. The MEP gradient view was displayed by computing multipole-moment's calculations and it was used to justify the charge oriented static field potentials. The computational calculations were performed on the structure by HF methods B3LYP and B3PW91 with 6-31G (d, p) basis set. The electronic excitation energy absorption peak was observed and the peaks were assigned for transitions.

4. RESULT AND DISCUSSIONS

4.1. MOLECULAR GEOMETRY AND XRD ANALYSIS

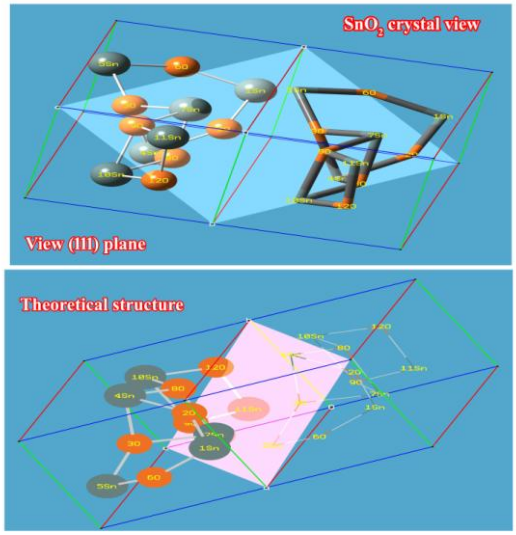

FIGURE 1
THE OPTIMIZED SIMULATED STRUCTURE OF THE SnO_2 WAS OBTAINED FROM GAUSSIAN 09 AND GAUSS VIEW PROGRAM

Single molecule of SnO_2 posses a symmetry top molecular structure and due to its in multi coordinates molecular arrangement, it was belong to C_S point group symmetry. The optimized simulated structure of the SnO_2 was obtained from Gaussian 09 and Gauss view program which was shown in Figure 1. The basic theoretical crystal structure in (111) plane view was displayed in the Figure in which dual merged crystal system also viewed. The structure was optimized well and the zero point Vibrational energy of the compound in HF with 6-31G(d,p) at different annealing temperatures (200º, 400º and 600º) were 16.5, 15.76 and 14.33 kcal/mol, respectively. The ground level optimized energy was decreased when it is going from lower annealing temperature to higher temperature. The observed view inferred that, when the particle size reduced and simultaneously, the zero point energy also decreased.

Since the present nano crystal was composed of multi Sn-O bonds in different planes, these bonds forced to have different bond length. The bond length of Sn_1-O_2 and Sn_1-O_6 were 1.930 Å and 1.953Å for respectively whereas the bond length of Sn_1-O_3 was found to be 3.67Å. This enormous difference among these bond lengths was mainly due to that, the first two bonds located in 'a' plane while last bond situated in 'c' plane. The Sn-O bond length at all the places getting reduced due to the application of annealing temperatures; in the case of Sn1-O2 and Sn1-O6, the bond lengths were 1.930Å & 1.953Å, 1.915 & 1.938Å and 1.911Å & 1.934Å at 200º, 400º and 600º respectively. In reverse order, the bond length O3-Sn4, O3-Sn5, O3-Sn7, O8-Sn10, O9-Sn10 and O9-Sn11 were appeared to be 2.155Å, 2.001Å, 2.065Å, 2.055Å, 2.142Å and 2.027Å respectively. Here, the bond lengths were not differed much among them and this was mainly by the existence of bonds in inter-planes. These bond lengths were also getting reduced due to the temperatures. The bond angle of O2-Sn1-O3 and O3-Sn1-O6 at same planes was calculated to be 44.7º and 47.44º respectively whereas the bond angle of Sn1-O2-Sn4, Sn1-O3-Sn4 and Sn1-O3-Sn5 were computed to be 142.4º, 73.2º and 75.3º respectively. The bond angle of first group was observed to be smaller than second group since the existence of first set bond angle at (100) & (200) planes while the second set placed at (111), (110) and (220) planes. These planes were also getting elevated due to the annealing temperatures which were presented in the Table 1.

Geometrical Parameters	HF/6-311+G(d,p)		
	200°C	400°C	600°C
Bond length(Å)			
(Sn1-O2)	1.930	1.915	1.911
(Sn1-O3)	3.679	3.650	3.643
(Sn1-O6)	1.953	1.938	1.934
(O2-Sn4)	1.967	1.951	1.948
(O3-Sn4)	2.155	2.138	2.133
(O3-Sn5)	2.001	1.986	1.982
(O3-Sn7)	2.065	2.049	2.045
(Sn5-O6)	1.916	1.901	1.897
(Sn7-O8)	2.046	2.030	2.026
(Sn7-O9)	2.053	2.037	2.033
(Sn7-O12)	3.874	3.843	3.836
(O8-Sn10)	2.055	2.039	2.035
(O9-Sn10)	2.142	2.126	2.121
(O9-Sn11)	2.027	2.011	2.007
(Sn11-O12)	1.928	1.913	1.909
Bond angle(°)			
(O2-Sn1-O3)	44.784	44.434	44.345
(O3-Sn1-O6)	47.448	47.078	46.983
(Sn1-O2-Sn4)	142.468	141.357	141.072
(Sn1-O3-Sn4)	73.274	72.703	72.556
(Sn1-O3-Sn5)	75.302	74.715	74.564
(Sn1-O3-Sn7)	86.202	85.529	85.357
(Sn4-O3-Sn5)	123.990	123.023	122.775
(Sn4-O3-Sn7)	96.205	95.455	95.262
(Sn5-O3-Sn7)	126.503	125.516	125.263
(O2-Sn4-O3)	80.970	80.338	80.176
(O3-Sn5-O6)	89.655	88.955	88.776
(Sn1-O6-Sn5)	147.580	146.429	146.133
(O3-Sn7-O8)	76.002	75.409	75.257
(O3-Sn7-O9)	100.074	99.293	99.093
(O3-Sn7-Sn1O2)	114.565	113.672	113.443
(O8-Sn7-O9)	76.074	75.480	75.328
(O9-Sn7-Sn1O2)	34.362	34.094	34.025
(Sn7-O8-Sn10)	106.387	105.557	105.344
(Sn7-O9-Sn10)	103.008	102.204	101.998
(Sn7-O9-Sn11)	122.505	121.549	121.304
(Sn10-O9-Sn11)	99.261	98.487	98.288
(O8-Sn10-O9)	73.940	73.363	73.215
(O9-Sn11-O12)	77.147	76.546	76.391
(Sn7-O12-Sn11)	92.232	91.513	91.328

TABLE 1
OPTIMIZED GEOMETRICAL PARAMETERS FOR SnO_2 ANNEALED AT 200º-600º C

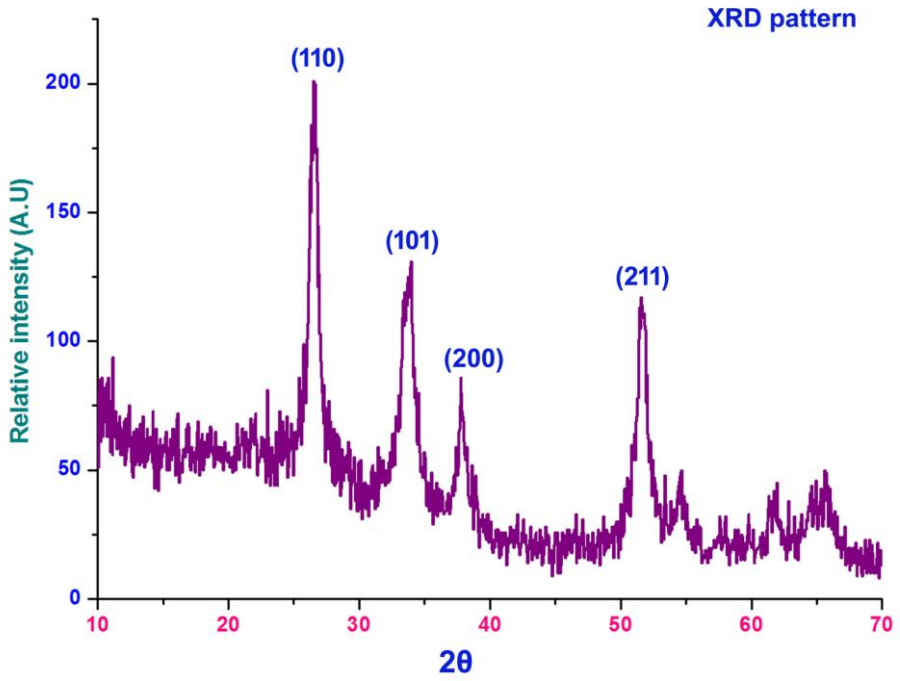

FIGURE 2
THE OBTAINED XRD PATTERNS FOR THE PREPARED AS WELL AS THE ANNEALED SAMPLES AT 200º, 400º AND 600º C

The obtained XRD patterns for the prepared as well as the annealed samples at 200º, 400º and 600º C were seen in the Figure 2. The diffraction peaks were observed from the planes of (110), (101), (200) and (211) at 27º, 34º, 38º and 52º respectively. By the observation of peaks with maximum intensity, it was showed that, these planes were active which confirmed tetragonal crystalline phase. The lattice constant 'a' was found to be increased from 4.721 to 4.791 Å whereas 'c' decreased from 3.227 to 3.173 Å. The results also described the lengths of the tetragonal geometry and this observed data was validated by previous work [11].usually, the lattice expansion due to the adverse effect of micro strain and dislocation density by the application of O vacancy. The crystal size (D) was computed with the help of Scherer equation and it was estimated to be 36 nm. The x-ray peaks acquired from the active planes noted above which was supported by the computational geometry of the material. Such a reflective crest obtained from the active planes at annealing temperatures was retained.

4.2. MULLIKEN CHARGE ANALYSIS

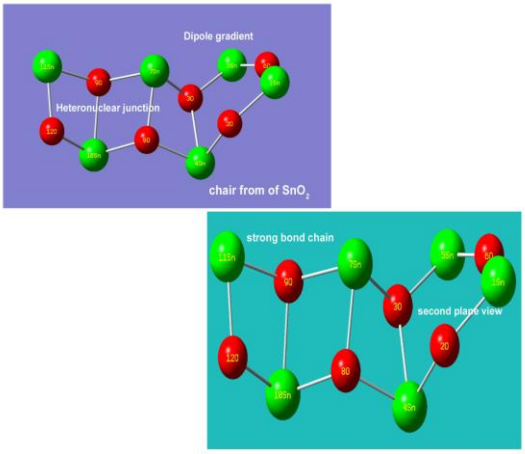

FIGURE 3
MULLIKEN CHARGE DISTRIBUTION

The Mulliken charge distribution was presented in the Figure 3 where due to the strong dipole character of core bonds Sn-O viewed in green and red color of atoms. The chain of alternative Sn and O atoms arranged in translational order to form the chain of SnO_2 material. Here, the O was highly electronegative whereas Sn was highly protopositive and both combined to initiate strong resultant dipole moment. Basically, at molecular level, it was found to be chair form structure and combined in different plane constructed the 3-D tetragonal lattice. The strong dipole character of individual molecule was causing the consistent crystalline semiconducting material.

4.3. VIBRATIONAL ANALYSIS

4.3.1. VIBRATIONAL ASSIGNMENTS

The molecular structure of SnO_2 material belongs to C_S point group symmetry due to the existence Sn-O bonds in different planes. The entire structure was contained 12 atoms and according to the vibrational rules of cyclic molecule, 30 vibrational modes were obtained in which 12 stretching modes, 9 in plane and 9 out of plane bending modes were observed.

$$\Gamma_{vib} = 21' + 9A''$$

In this case, the FT-IR and FT-Raman spectra have been recorded at macro and nano phase of the SnO_2 materials. On the spectral sequence, the active IR and Raman peaks were observed. The spectral wavenumbers were found to be active below the mid IR region and due to this reason; the spectral scan was repeated different times and finally the active bands were recorded. The experimental vibrational wavenumbers in the form of FT-IR and FT-Raman frequencies for various modes of vibrations have been presented in Table 2. The recorded spectra of the present metal oxide were displayed in the Figures 4 and 5 respectively.

TABLE 2
CALCULATED FREQUENCIES OF SnO_2 IN REDUCED NANO LEVEL

S. No.	Experimental frequency		Calculated frequency	Vibrational assignments
	FT-IR	FT-Raman		
1	710w	710s	942	(Sn-O)υ asym
2	-	690s	874	(Sn-O)υ asym
3	-	610m	791	(Sn-O)υ asym
4	600w	-	748	(Sn-O)υ asym
5	580w	580s	706	(Sn-O)υ asym
6	560s	560w	697	(Sn-O)υ sym
7	540vs	540s	613	(Sn-O)υ sym
8	510m	510s	580	(Sn-O)υ sym
9	480vs	-	503	(Sn-O)υ sym
10	440m	-	489	(Sn-O)υ sym
11	400vs	400w	430	(Sn-O)υ sym
12	395w	-	419	(Sn-O)υ sym
13	370s	370w	412	(O-Sn-O) δ
14	360s	360w	378	(O-Sn-O) δ
15	330m	-	364	(O-Sn-O) δ
16	310m	310w	285	(O-Sn-O) δ
17	-	290w	271	(O-Sn-O) δ
18	280w	-	245	(O-Sn-O) δ
19	-	260w	219	(O-Sn-O) δ
20	-	240w	180	(O-Sn-O) δ
21	220w	-	168	(O-Sn-O) δ
22	200w	200w	145	(O-Sn-O) δ
23	180w	180w	138	(O-Sn-O) γ
24	170w	-	108	(O-Sn-O) γ
25	160w	160w	105	(O-Sn-O) γ
26	150w	-	82	(O-Sn-O) γ

27	140w	-	71	(O-Sn-O) γ
28		130w	40	(O-Sn-O) γ
29	110w	-	29	(O-Sn-O) γ
30	100w	-	22	(O-Sn-O) γ

vs; very strong, s; strong, m; medium, w; weak, vw; very weak. υ; stretching, δ; in plane bending: γ-out of plane bending

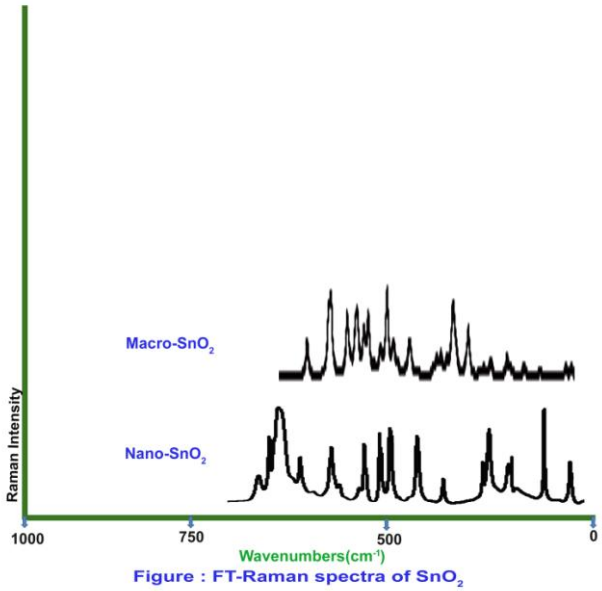

FIGURE 4
SPECTRA OF THE PRESENT METAL OXIDE

4.2.2. Sn-O VIBRATIONS

The present metal oxide compound has number of Sn-O bonds in different planes ad all were found to be present whereas some those vibrations were appeared to be active in IR and simultaneously inactive in Raman according to the mutual exclusion principle. Here, the spectral pattern was recorded at macro and nano level of material and the vibrational pattern at nano level was found to be active and with very strong intensity than at macro level. At that level, the observed frequencies lagging somewhat when compared with nano level.

The vibrational modes related to many metal oxides with one or more one oxygen atom usually absorb in the region 1020 - 970 cm^{-1}[12-13]. Particularly, the Sn-O vibrational pattern is observed in the region of 780-580 cm^{-1}[14-15]. In this vibrational region, the stretching frequencies are usually found well above 610 cm^{-1} whereas the bending modes are observed well below 600 cm^{-1}. In this case, the asymmetric Sn-O stretching bands were obtained at 710, 690, 610, 600 and 580 cm^{-1} and symmetric stretching bands were found at 560, 540, 510, 480, 440, 400 and 395 cm^{-1}. Here, the asymmetric stretching vibrations were observed almost within the expected limit whereas the symmetric vibrations were shifted well below the allowed region of the metal oxide vibrations. The entire asymmetric vibrational bands of Sn-O bonds were found to be located at (110), (101), (200) and (211) planes which was supported by the XRD studies. The entire symmetric bands were moved down to well below the expected region due to their related bonds located subsequent planes. Correspondingly, the in plane and out of plane vibrations were appeared at 370, 360, 330, 310, 290, 280, 260, 240, 220 and 200 cm^{-1} and 180, 170, 160, 150 and 140 cm^{-1} respectively. Here, the entire bending modes were shifted to lattice vibrational region which was due to the lattice vibrational resonance effect.

4.3. FRONTIER MOLECULAR PROFILE

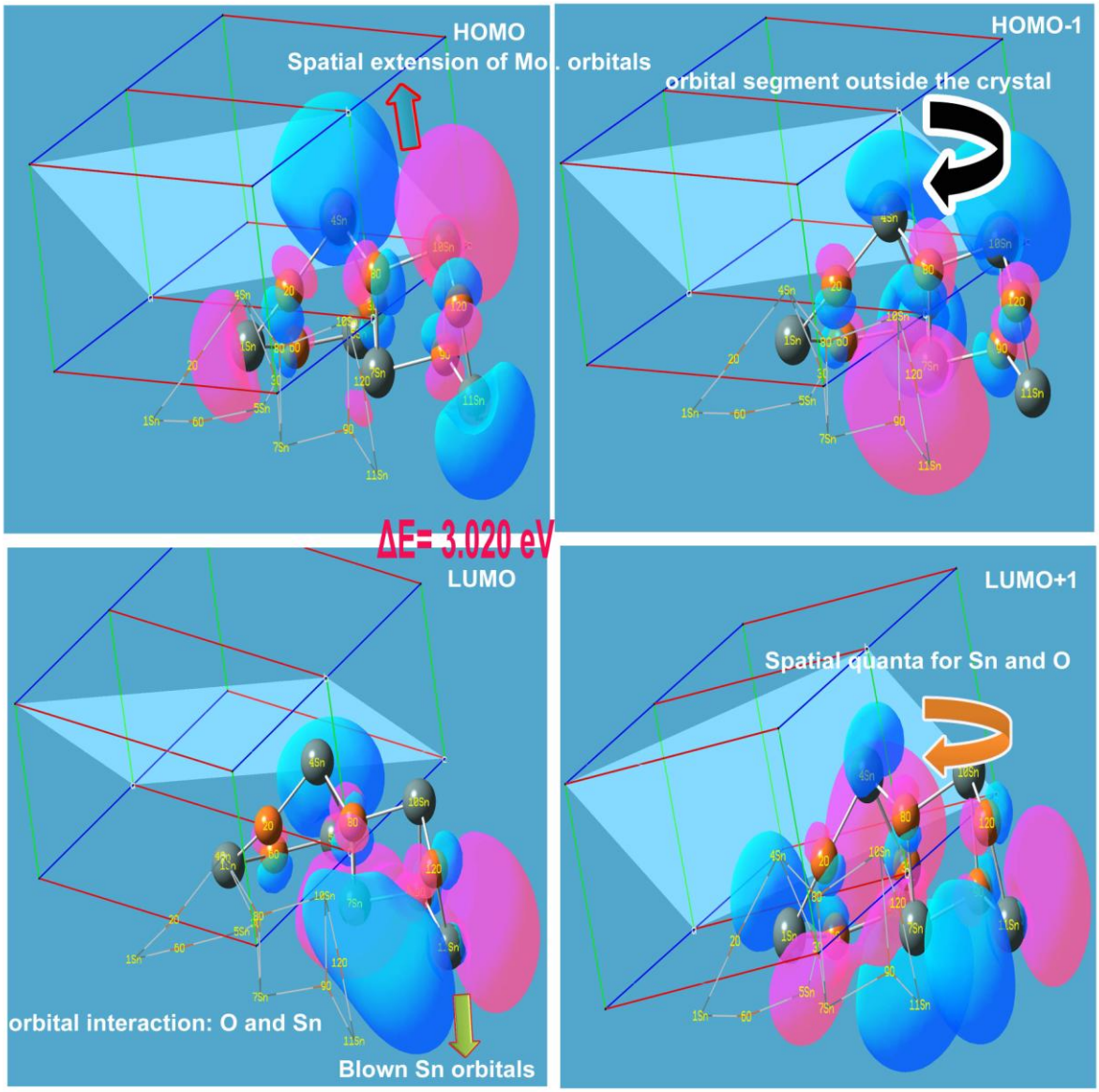

FIGURE 6
EXCITED AND NORMAL ORBITAL ARRANGEMENT

The frontier molecular orbital analysis is generally displaying the molecular orbital overlapping arrangement which is used to determine the molecular behavior for constructing the molecular orbital overlapping to share the electronic energy to produce semiconducting property in the material. The present nano material is a semiconductor and its semiconducting property can be described by the arrangement of HOMO and LUMO. The molecular setup in the material enabling the molecular reactivity to construct finite kubo gap which causing transducer action. The LUMO was appeared to be covering the Sn-O bond which was on the surface of the crystal system. The orbital interaction taking place over the surface bonds and their orbitals found to be blown and their electron is able to receive the energy which is linked on the surface. The HOMO was appeared over the area of the Sn-O bonds inside the crystal where the Sn-O orbitals overlapped and their associated electron cloud was found to be ready to produce transitions to vacant orbital system. This excited and normal orbital arrangement was presented in the Figure 6 where in which the spatial orbital extension becomes visible. This molecular setup rearranged narrow band gap which will be helpful to produce semiconducting property. Accordingly, the band gap of this compound was found to be 3.020 eV which was very narrow band gap and is able to receive the energy in wide range. In the next level of HOMO and LUMO, the cascading process was extended and the overlapping orbitals viable for arranging the semiconducting property as well.

.4. MEP VIEW ANALYSIS

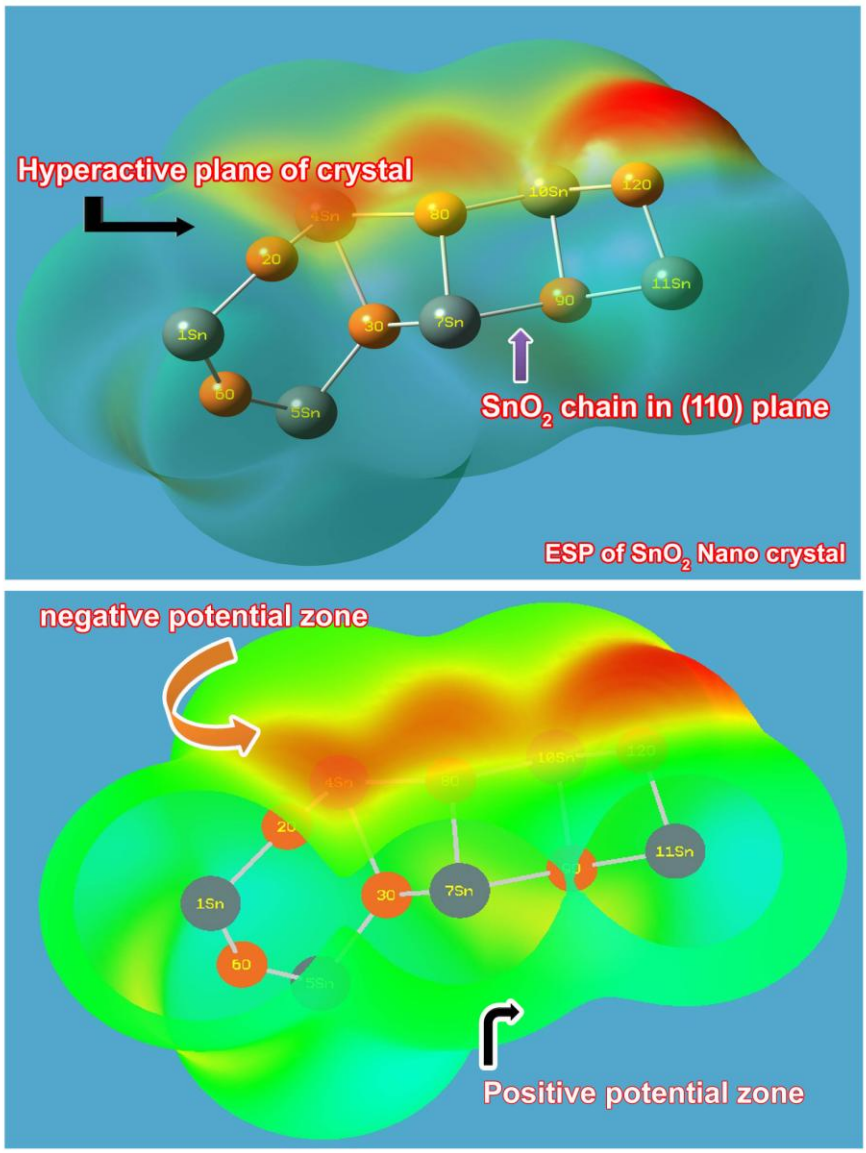

FIGURE 7
THE O WAS HAVING ELECTROPHILIC CAPABILITY WHILE THE Sn GROUP OF ATOMS HAS NUCLEOPHILIC POTENTIAL GRADIENT

The molecular electrostatic potential was stimulated within the molecular system by the existence of strong dipole moment in inter-connecting loop. The opposite potential was displaced with respect to the charge depletion between electrophilic and nucleophilic region. Here, the O was having electrophilic capability while the Sn group of atoms has nucleophilic potential gradient which was shown in the Figure 7. The electrophilic link region was found to be appeared as red path way on molecular structure while the nucleophilic domain was appeared over Sn atoms in the material. The blue and red color gradient showed the charge depletion on Sn-O bonds on (110) plane where the electrostatic potential was enriched. The hyper active potential was generated on Sn-O sites which enabling the semiconducting property.

4.5. EDAX SPECTRAL STUDIES

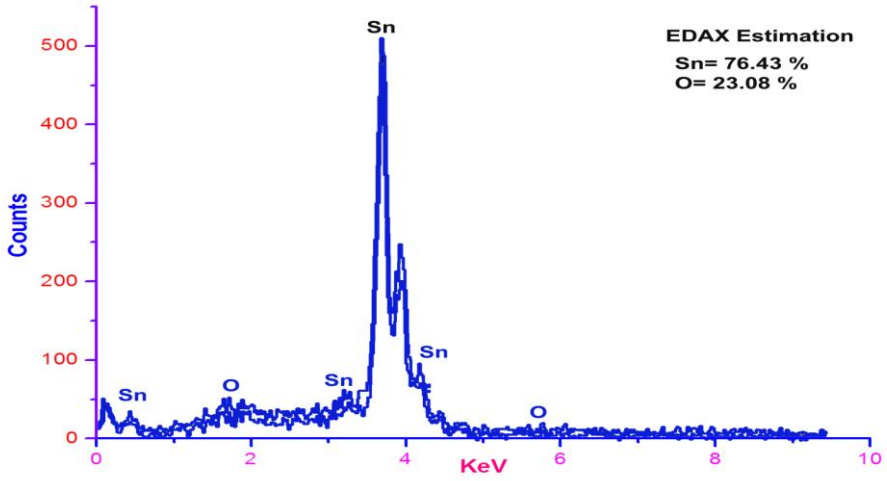

FIGURE 8
THE EDAX ESTIMATION DEFLECTION PEAKS

The EDAX estimation deflection peaks were shown in Figure 8 where the signals were available that corresponding to compositional elements of SnO_2 nano material. The graph was obtained between counts and energy of energy dispersive spectrum. It is an effective tool which has analytical capability to measure the ratio of the compositional parts of the material. The graph showed the maximum intensity signal which was assigned to the Sn metal and other associated peaks illustrated the presence of O in the interstitial positions in the Sn lattice. The observed results determined the ration of the Sn and O compositions and such that the presence of Sn was calculated to be 76.43% and O was 23.058%. This stoichiometric ratio was ensured observed data which was capable to make reaction mechanism in the nano materials. The experimentally obtained peaks showed the purity of the nano material and it was not contaminated by any other materials. The band gap of the materials at different temperatures was predicted and was shown in the form of graph which was displayed in the Figure 9. For the present case, the band gap was getting reduced from 3.94 eV at 100º C and stabilized at 3.43 eV in 600º C. This was effective band gap which is opting for measuring toxic gas wavelength and it was also found to be synchronized with optical region.

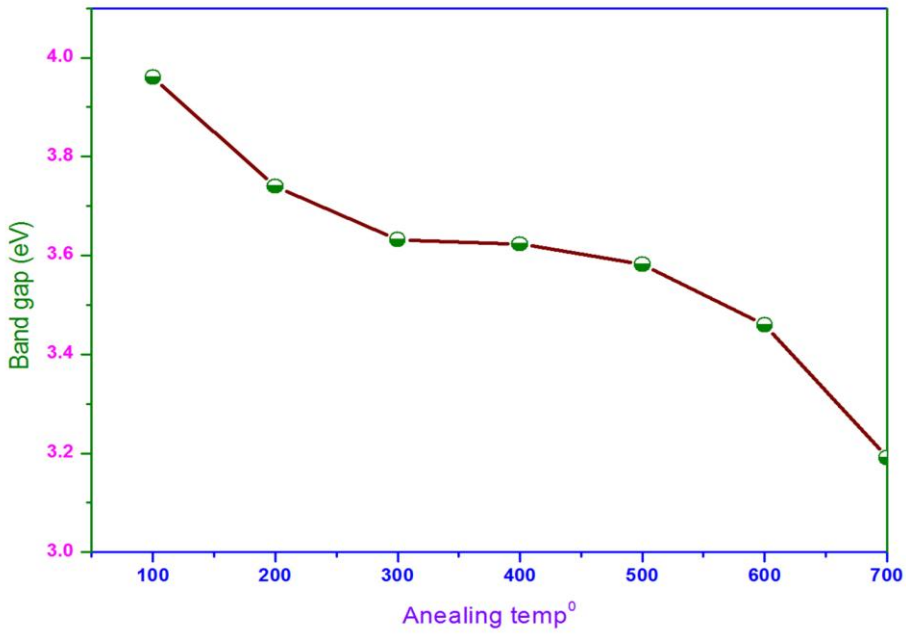

FIGURE 9
BAND GAP OF THE MATERIALS AT DIFFERENT TEMPERATURES

4.6. XPS SPECTRAL ANALYSIS

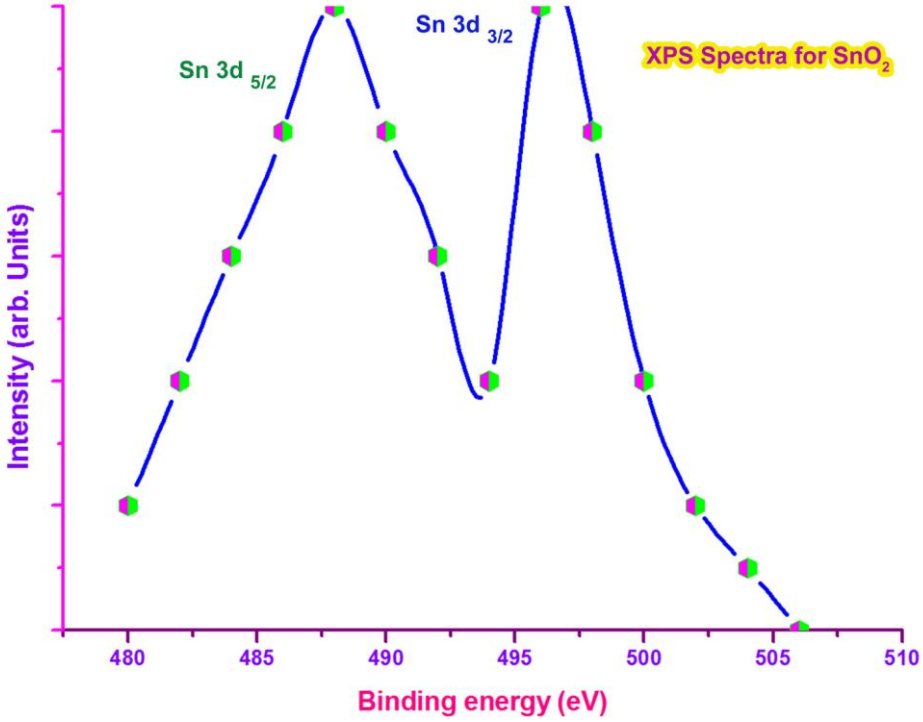

FIGURE 10
SnO_2 MATERIAL WERE ATTAINED BY XPS PROFILE AND THE ASSOCIATED SPECTRUM

The XPS data provide the precious quantitative and chemical energy state information from the topographical surface of the material. The intensity of a photoelectron peak and the binding energy were used to measure the quantity of detected element. The chemical compositions and energy state of the present case; SnO_2 material were attained by XPS profile and the associated spectrum was noticed in the Figure 10. The Figure of x-ray photoelectron spectrum showed the presence of elements in the nano material. The Sn and O compositions were appeared as spin orbit doublet such as Sn $3d_{3/2}$ and $3d_{5/2}$ at 497.2 eV and 487.5 eV respectively. The observed d-orbital energy doublet depicted the energy association of Sn nano materials. The experimentally obtained result was closely related to XRD as well as EDS data and the results was conformed that, the SnO_2 material able to have good chemical responsibility and electrostatic performance.

4.7. HYPER OPTICAL ACTIVITY ANALYSIS

As the polarizability and hyperpolarizability of the nano crystal is facilitated to examine the optical sensitivity, such the parameters to be analyzed for studying optical sensitiveness of nano materials. It is also used to estimate the magneto-optical response of the nano material [16]. The calculated diagonal polarizability and hyperpolarizability parameters for SnO_2 nano material were presented in the Table 3. For this case, the total and average polarizability have been computed to be 253.56 $x10^{-33}$esu and 184.36 $x10^{-33}$esu respectively, which were precise and such that the values showed inducement of enriched optical polarization path in the present nano material. The able optical path was breeding the effect of second and third harmonic generation. Thus, the SnO_2 nano material is identified to be used to fabricate optical doubler device.

TABLE 3
THE DIPOLE MOMENTS μ (D), THE Polarizability *α*(a.u.), THE AVERAGE POLARIZABILITY α_o (esu), THE Anisotropy Of The Polarizability Δα (esu), And The First Hyperpolarizability β(esu) OF NANO SnO_2

Parameter	a.u.
α_{xx}	184.2
α_{xy}	10.84
α_{yy}	192.25
α_{xz}	2.12
α_{yz}	2.36
α_{tot}	184.36
$\Delta\alpha$	253.56
μ	3.81
β_{tot}	1163.110

It was early recognized that, the hyperpolarizability element is effective parameter for ensuring hyper active optical characteristics in the nano material and also it is nonlinear optical behavior which generates new photon process by interacting photon energy at lattice site. Here, it was calculated to be 1163.110 $x10^{-33}$esu which was more than sufficient to produce nonlinear optical activity. When compared with thiourea material, the nonlinear effect was found to be four times greater. In addition to that, its dipole moment was found to be 3.81 which was very high to deplete the charge levels inside the nano material and it emphasized the fascinated electro-optical response.

5. CONCLUSION

The nano material; SnO_2 under investigation was thoroughly characterized by experimental and theoretical tools. Some of the important properties were studied well using computational theories. By carrying out morphological, optical, vibrational, photo-electrical and magneto-optical studies, the multidimensional characteristics of the materials were studied. The vibrational studies was solved the x-ray reflections at different important planes of crystal. After completing this work, it was determined that, the unknown properties as well as unknown applications of SnO_2. By synthesize the SnO_2 nano material using suitable method in appropriate conditions, the entire above said properties can be extracted. The present synthesized SnO_2 nano compound was able to have gas sensing as well as opto-electronic properties primarily and it was found to be capable to double the optical frequencies.

REFERENCES

1. Hui Pan and Yuan Ping Feng, ACS Nano, *2* (11), (2008), 2410–2414.
2. G.C. Hadijipanyis., R.W. Siegel, Nanophase materials, 4 (1994) 121.
3. A. Ayeshamariam, C.Sanjeeviraja, R. Perumal Samy, Journal on Photonics and Spintronics, 2, 2(2013), 4-8.
4. W. Dazhi, W. Shulin, C. Jun, Z. Suyuan, L. Fangqing, Phys. Rev. B, 49 (1994) 282.
5. J.R. Brown, P.W. Haycock, L.M. Smith, A.C. Jones, E.W. Williams, Sensors and Actuators B 63 (2000) 109.
6. F. Gu, S.F. Wang, M.K. Lu, Journal of Crystal Growth 255, (2003), 357.
7. A. Ayeshamariam, S. Ramalingam, M. Bououdina, M. Jayachandran, Spectrochimica Acta Part A: Molecular and Biomolecular Spectroscopy 118 (2014) 1135-1143.
8. Raziyeh Arab Ahmadi and Saeid Amani, Molecules, (2012), 17, 6434-6448.
9. Gaussian 09, Revision D.01, M. J. Frisch, G. W. Trucks, H. B. Schlegel, G. E. Scuseria, M. A. Robb, Gaussian, Inc., Wallingford CT, 2016.
10. James B. Foresman, Aeleen Frisch, Exploring Chemistry with electronic structure methods, Second edition, Gaussian Inc., Pittsburgh, (2009).
11. Iqbal, M. Zubair; Wang, Fengping; Hussain, Riaz; Iqbal, Tahir; Ali, Israt; Rafique, M. Yasir; Ali, Shujjat, 6;7, (2014),791-796.

12. A. Cadsen, Infrared Spectra of Minerals and Related Inorganic Compounds, Butterworth. London. (1975).
13. S. D. Ross, Inorganic Infrared and Raman Spectra, McGraw- Hill, London, (1972).
14. K. Nakamoto, Infrared and Raman Spectra of Inorganic and Coordination Compounds, 5^{th} edn, Wiley, New York, (1997).
15. J. Zuo, C. Xu, X. Liu, C.Wang, C.Wang, Y. Hu, Y. Qian, J. Appl. Phys. 75 (3) (1994) 1835–1836.
16. Jurgen Gauss. Molecular Properties. In J. Grotendorst, editeur, Modern Methods and Algorithms of Quantum Chemistry, volume 3 (2000), 541–592.